© Pol J Radiol 2026; 91: e124-e131
DOI: https://doi.org/10.5114/pjr/215289

Received: 30.08.2025
Accepted: 08.12.2025
Published: 10.03.2026

Polish Journal of Radiology
http://www.polradiol.com

Original paper

Intravoxel incoherent motion diffusion-weighted imaging in the staging of rectal non-mucinous adenocarcinoma

Yunus Yasar[1,A,B,C,D,E,F,G], Fatma Kulali[1,A B,C,D,E,F,G], Ozgul Duzgun[2,A,B,C,D], Yasar Bukte[1,A,B,C,D]

[1]Department of Radiology, Umraniye Training and Research Hospital, University of Health Sciences, Istanbul, Turkey
[2]Department of General Surgical Oncology, Umraniye Training and Research Hospital, University of Health Sciences, Istanbul, Turkey

Abstract

Purpose: To investigate the role of intravoxel incoherent motion diffusion-weighted imaging (IVIM-DWI) in the prediction of histological differentiation and local invasion (T stage) of rectal non-mucinous adenocarcinoma for appropriate treatment planning.

Material and methods: Pre-operative magnetic resonance imaging (MRI) and IVIM-DWI examinations were prospectively performed in patients with rectal non-mucinous adenocarcinoma. A total of 36 patients with a mean age of 61 ± 8 years (range: 26-85 years) were included. Size, signal intensities and enhancement pattern of tumors, lymphadenopathy, serosal involvement, adjacent organ invasion, and metastasis were noted. IVIM-DWI parameters were estimated. Relationships between IVIM-DWI parameters and histopathological results were analyzed using Mann-Whitney *U* and Kruskal-Wallis tests. Receiver operating characteristic analysis was performed for optimal cut-off values.

Results: In our study, a total of 36 patients were enrolled. There was a negative relationship between tumor differentiation and perfusion (*f*) ($p < 0.05$). A negative relationship was detected between T staging and true diffusion (*D*), pseudo-diffusion coefficient (D^*) and apparent diffusion coefficient (*ADC*) values ($p < 0.05$). Lower *D*, D^*, and *ADC* values were detected in late stage (T3-T4) rectal tumors and nodal metastasis ($p < 0.05$). Lower f values were achieved in higher histological grades ($p < 0.05$). In differentiation of poorly from well- and moderately differentiated tumors, cut-off value of < 20.89 showed 88.5% sensitivity and 85.7% specificity (area under the curve: 0.771, $p < 0.05$).

Conclusions: Aggressive tumors with low histological differentiation and metastatic lymphadenopathy exhibit lower diffusion and perfusion values. As a perfusion indicator, f provides valuable information regarding tumor differentiation. IVIM-DWI can be used as an adjunctive modality to routine abdominal MRI in the local staging of rectal carcinoma.

Key words: rectal cancer, staging, magnetic resonance imaging, lymph node, diffusion-weighted imaging, intravoxel incoherent motion.

Introduction

Rectal cancer accounts for approximately one-third of all colon cancers [1]. In rectal cancer, the five-year survival rate reaches about 90-100% because of improved surgical techniques, increased options in chemoradiotherapy, advancing imaging methods, and rising diagnostic performance [2,3]. Moreover, the prognosis of rectal cancer and treatment planning are based on various factors, including tumor extension, the presence of lymphadenopathy, and the histological grade of the tumor [4,5].

Endoscopy is required for histopathological diagnosis of rectal cancer, whereas it has several limitations in demonstrating the depth of tumoral involvement and adjacent

Correspondence address:
Fatma Kulali, Department of Radiology, Umraniye Training and Research Hospital, University of Health Sciences, 1 Adem Yavuz St., 34764 Istanbul, Turkey, e-mail: ftkulali@gmail.com

Authors' contribution:
A Study design · **B** Data collection · **C** Statistical analysis · **D** Data interpretation · **E** Manuscript preparation · **F** Literature search · **G** Funds collection

organ invasion. Therefore, magnetic resonance imaging (MRI) is a valuable preoperative imaging modality for the evaluation of local invasion and staging [4,6]. The tumor's morphological features are precisely depicted on MRI. Moreover, diffusion-weighted imaging (DWI) provides assessment of functional and microstructural characteristics. DWI with quantitative measurements contributes to the prediction of the histopathological properties of the tumor and the prognosis of the patient [4,7,8]. Nevertheless, microcirculation, in addition to the diffusion of water molecules, influences conventional DWI parameters.

Intravoxel incoherent motion DWI (IVIM-DWI) can differentiate water diffusion from microcapillary perfusion. In IVIM-DWI, four parameters can be estimated: the apparent diffusion coefficient (*ADC*); true diffusion (*D*), reflecting free water molecule movement in the extracellular space; the pseudo-diffusion coefficient (*D**), which shows microcapillary perfusion; and the perfusion fraction (*f*) [9,10]. Several studies in the literature highlight the importance of IVIM-DWI for the staging of various tumors and estimation of their histological behaviors, as well as the evaluation of treatment response [11-15].

Therefore, we aimed to investigate the role of IVIM-DWI in estimating histological differentiation grade and local invasion (T stage) in rectal non-mucinous adenocarcinoma to predict prognosis and support appropriate treatment planning.

Material and methods

Patients

The institutional ethics committee approved this prospective study. Written informed consent of all patients was obtained. Between July 2018 and May 2019, 39 consecutive patients with non-mucinous rectal adenocarcinoma who were diagnosed by endoscopic biopsy were referred for pre-operative MRI examination. Two patients with cardiac pacemakers and one patient with a femur prosthesis artifact were excluded. A total of 36 patients with non-mucinous rectal adenocarcinoma underwent pre-operative abdominal MRI and IVIM-DWI examination in our study. All patients had a pre-operative endoscopic biopsy.

MRI and IVIM-DWI protocol

All patients underwent MRI on a 1.5-Tesla MRI system (Optima MR450w, GE Healthcare, Milwaukee, USA).

The imaging protocol used for upper abdominal MRI in the study consisted of coronal T2-weighted single-shot fast spin-echo (SS-FSE) (field of view [FOV]: 400 mm, slice thickness: 8 mm, slice gap: 1 mm, repetition time [TR]: 4000 ms, echo time [TE]: 90 ms, matrix: 320 × 224), axial T2-weighted SS-FSE (FOV: 410 mm, slice thickness: 6 mm, slice gap: 1 mm, TR: 4000 ms, TE: 90 ms, matrix: 320 × 224), axial fat-suppressed T2-weighted SS-FSE (FOV: 410 mm, slice thickness: 6 mm, slice gap: 1 mm, TR: 4000 ms, TE: 90 ms, matrix: 320 × 224), axial dynamic pre- and post-contrast T1-weighted three-dimensional (3D) spoiled gradient echo liver acquisition with volume acceleration (LAVA) (FOV: 256 mm, slice thickness: 5.6 mm, TE: 2.1 ms, TR: 6.6 ms, matrix: 256 × 192), post-contrast coronal T1-weighted 3D LAVA (FOV: 430 mm, slice thickness: 5 mm, TE: 2.1 ms, TR: 6 ms, matrix: 320 × 224), and axial DWI sequence (FOV: 410 mm, slice thickness: 6 mm, slice gap: 1 mm, TE: 82 ms, TR: 6000 ms, matrix: 96 × 128, number of excitations: 4).

The imaging protocol used for lower abdominal MRI in the study consisted of sagittal T2-weighted periodically rotated overlapping parallel lines with enhanced reconstruction (PROPELLER) (FOV: 330 mm, slice thickness: 5 mm, slice gap: 1.5 mm, TR: 2643 ms, TE: 90 ms, matrix: 256 × 256), coronal T2-weighted PROPELLER (FOV: 400 mm, slice thickness: 5 mm, slice gap: 1.5 mm, TR: 6115 ms, TE: 71 ms, matrix: 256 × 192), axial T2-weighted fast relaxation fast-recovery fast spin-echo (FR-FSE) (FOV: 430 mm, slice thickness: 5 mm, slice gap: 1.5 mm, TR: 7773 ms, TE: 110 ms, matrix: 256 × 192), axial T1-weighted spin-echo (FOV: 430 mm, slice thickness: 5 mm, slice gap: 1.5 mm, TR: 744 ms, TE: 23.5 ms, matrix: 256 × 192), pre- and post-contrast axial T1-weighted 3D LAVA (FOV: 430 mm, slice thickness: 5 mm, TE: 2.1 ms, TR: 6.6 ms, matrix: 256 × 192), and axial IVIM-DWI sequence (FOV: 380 mm, slice thickness: 5 mm, slice gap: 1 mm, TE: 78 ms, TR: 4000ms, matrix: 80 × 128).

Total scan time for IVIM-DWI was approximately 3-4 min. IVIM-DWI acquisition was performed in the axial plane by applying diffusion-sensitive gradients in all three directions (x, y, z) using a breath-hold single-shot turbo spin-echo echo-planar imaging (SS-TSE-EPI) sequence at 11 different *b* values (0, 50, 100, 150, 200, 400, 600, 800, 1000, 1200, 1500 s/mm^2). Isotropic images consisted of 'trace' images obtained by multiplying the signal intensities measured in x, y, and z directions to eliminate direction-dependent signal changes. ADC maps of isotropic images were created automatically.

Among patients who underwent operations (n = 18), abdominal MRI and IVIM-DWI examinations were performed 5 to 7 days before surgery. Patients who received neoadjuvant chemoradiotherapy were scanned at least two months after treatment completion. Because the aim of the study was not to analyze the impact of neoadjuvant treatment on intravoxel incoherent motion (IVIM) parameters, no separate subgroup analysis was performed.

Radiological and histological evaluation

The MRI and IVIM-DWI findings were investigated by two radiologists in consensus before surgery or neoadjuvant treatment. Evaluation and measurements were performed at the workstation (AW Volume Share 7, GE Healthcare, Milwaukee, USA), and IVIM data were processed in the

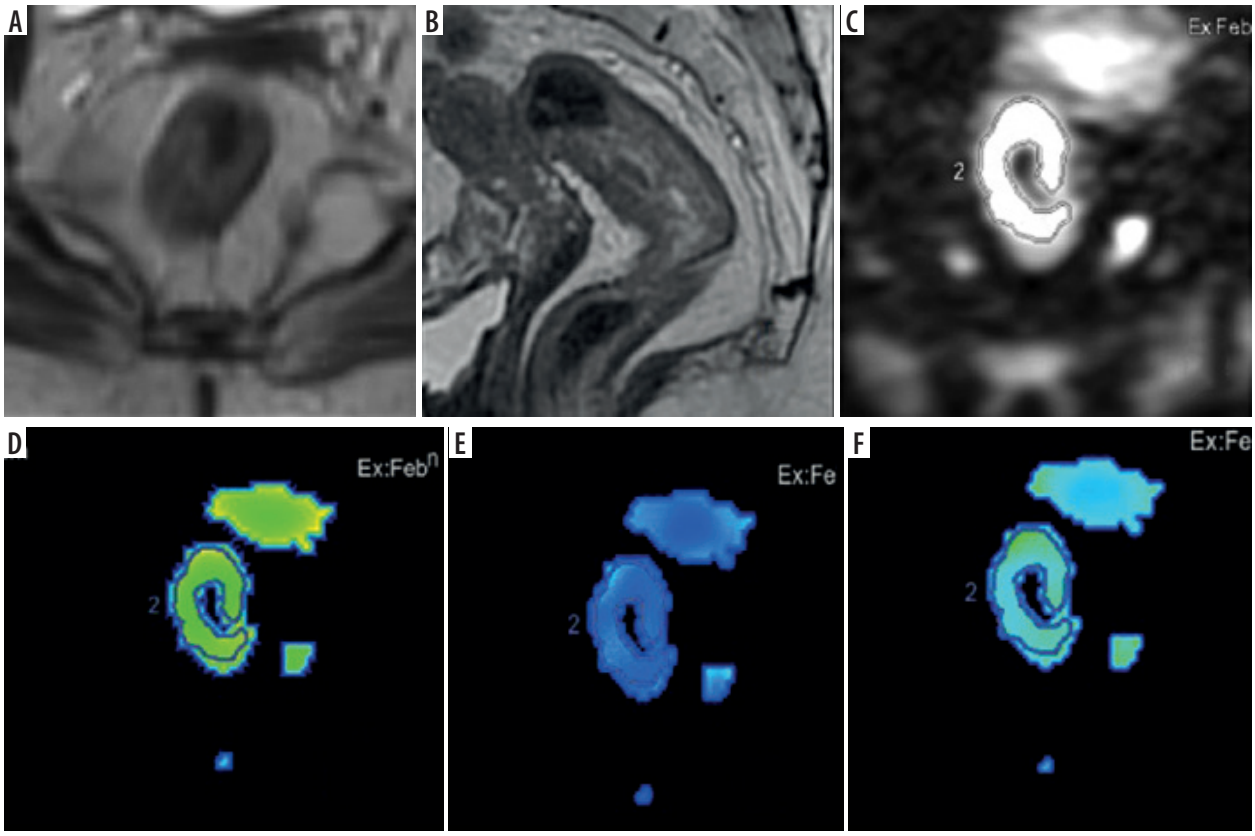

Figure 1. Axial (**A**) and sagittal (**B**) T2-weighted images, diffusion-weighted imaging (DWI) (**C**), and intravoxel incoherent motion-DWI parameter maps including true diffusion (**D**), pseudo-diffusion coefficient (**E**) and perfusion fraction (**F**) in a patient with rectal cancer

IVIM* (GE Healthcare, Milwaukee, USA) program. The maximum diameter, T1- and T2-weighted signal intensities, contrast enhancement pattern of rectal tumors, presence of lymphadenopathy, involvement of the serosa, adjacent organ involvement, features of lymph nodes (size, shape, contour), and distant metastases were noted.

In DWI, three consecutive region of interest (ROI) measurements were performed manually at the widest solid component of the tumor, with exclusion of cystic or necrotic components. The average of these three ROIs was estimated. *D*, *D**, *f*, and *ADC* values were calculated from each measurement (Figures 1 and 2).

All patients had biopsy-proven non-mucinous rectal adenocarcinoma. In patients who underwent surgical resection, the reference standard was surgical histopathology for evaluation of tumoral invasion and lymph node metastasis. In clinically inoperable patients demonstrating adjacent organ invasion on imaging, conventional MRI served as the reference standard for T4 staging and invasion assessment. Patients were classified according to histological differentiation, tumoral invasion depth, and the presence of pathological lymph nodes, based on histopathological results and conventional MRI. The comparison of histopathological results and MRI findings with IVIM-DWI parameters was analyzed statistically. Lymph node evaluation was performed using a lesion-based approach; each lymph node was analyzed individually and treated as a separate data point regardless of the number of nodes present within the same patient. Nonetheless, metastatic lymph node categorization was performed only in surgical patients. In patients with no malignant lymph nodes in the pathological specimen, lymph nodes > 0.5 cm on conventional MRI were considered benign. A malignant lymph node group was formed based on histopathological verification and the demonstration of metastatic lymph nodes on conventional MRI.

Statistical analysis

Statistical analyses were conducted using the Number Cruncher Statistical System 2007 software (Kaysville, Utah, USA). Descriptive statistical methods (mean, standard deviation, median, frequency, ratio, minimum, maximum) were employed to evaluate the study data, and the distribution of the data was assessed using the Shapiro-Wilk test. The Mann-Whitney *U* and Kruskal-Wallis tests were used to compare quantitative data between groups. Receiver operating characteristic (ROC) analysis was performed to identify the predictive values. The *p*-level < 0.05 was considered statistically significant.

Results

A total of 36 patients, composed of 20 men (56%) and 16 women (44%), were included in this study. The mean age was 61 ±8 years (range: 28-85 years).

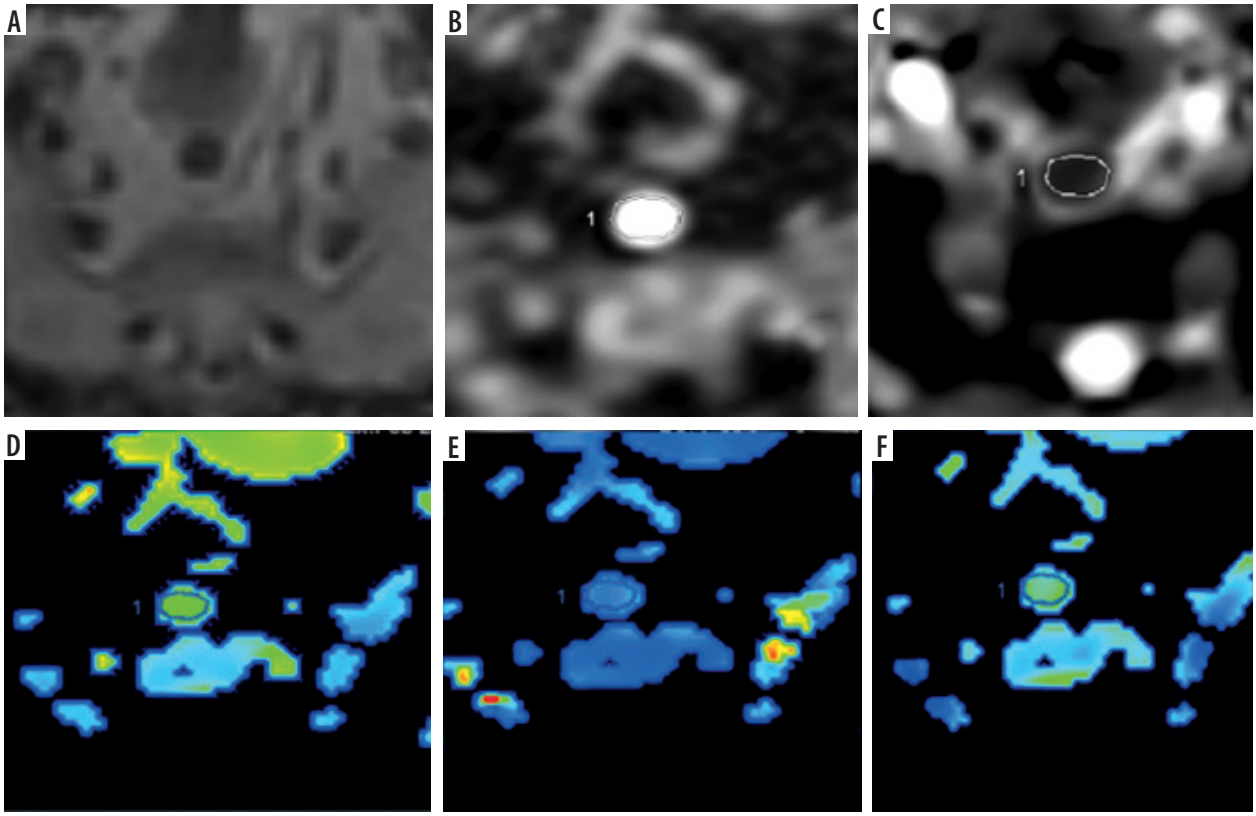

Figure 2. Axial T2-weighted image (**A**), diffusion-weighted imaging (DWI) (**B**), apparent diffusion coefficient map (**C**), and intravoxel incoherent motion-DWI parameter maps including true diffusion (**D**), pseudo-diffusion coefficient (**E**) and perfusion fraction (F) of metastatic lymphadenopathy in a patient with rectal cancer

Evaluation of IVIM-DWI parameters according to histological differentiation grade

All patients had biopsy-proven rectal non-mucinous adenocarcinoma with a known histological differentiation grade. The patients were classified into three groups according to histological differentiation: eight (22%) were poorly differentiated, 22 (61%) were moderately differentiated, and six (17%) were well differentiated. In comparison of IVIM parameters of rectal adenocarcinomas with known differentiation grades, a lower *f* value was achieved in the higher histological grade ($p < 0.01$). The mean *f* value in well-, moderately and poorly differentiated tumors was 31.86, 23.79, and 19.96, respectively (Table 1).

In differential diagnosis of well- and moderately differentiated tumors, the optimal cut-off value for the *f* parameter was 30, with 67% sensitivity, 100% specificity, positive predictive value of 64%, and negative predictive value of 96 (area under the curve [AUC]: 0.802 ± 0.125, $p < 0.05$) (Figure 3), whereas in differentiation of poorly differentiated tumors from well- and moderately differentiated tumors, the cut-off value of < 20.89 showed 88.5% sensitivity and 85.7% specificity (AUC: 0.771, $p < 0.05$).

Contribution of IVIM-DWI parameters to detection of adjacent organ invasion

In surgical patients ($n = 18$), the invasion degree was assessed from the surgical specimen. In the non-surgical patients, conventional MRI findings were evaluated by two radiologists, and adjacent organ invasion or perito-

Table 1. Statistical results of intravoxel incoherent motion parameters according to histological differentiation

Parameter	Well differentiated	Moderately differentiated	Poorly differentiated	*p**
D ($\times 10^{-3}$ mm^2/s)	1.169 ± 0.27	1.047 ± 0.19	1.139 ± 0.29	0.823
*D** ($\times 10^{-3}$ mm^2/s)	11.31 ± 2.36	12.00 ± 4.77	12.62 ± 4.18	0.294
f (%)	**31.86 ± 7.24**	**23.79 ± 4.78**	**19.96 ± 8.42**	**0.006**
ADC ($b = 1000$ mm^2/s) ($\times 10^{-3}$ mm^2/s)	1.55 ± 0.31	1.33 ± 0.27	1.34 ± 0.33	0.373
ADC ($b = 1500$ mm^2/s) ($\times 10^{-3}$ mm^2/s)	1.36 ± 0.28	1.17 ± 0.27	1.22 ± 0.32	0.577

*Kruskal-Wallis test; $p < 0.05$ was used to determine statistical significance

neal involvement was noted in nine patients. Among these patients, bladder (n = 4), prostate (n = 2), seminal vesicle (n = 1), uterus (n = 1), and adjacent peritoneum (n = 1) invasions were observed.

Among 27 patients, four had submucosal invasion (T1), two had muscularis propria invasion (T2), 11 had serosal and perirectal fatty tissue invasion (T3), and 10 had peritoneal or adjacent organ invasion (T4). T1 and T2 tumors formed early-stage tumors, and T3 and T4 tumors formed late-stage tumors (Table 2). In comparison of early-stage (T1-T2) and late-stage (T3-T4) tumors with respect to IVIM parameters, late-stage tumors showed significantly lower D, D^*, and ADC values ($p < 0.05$) (Table 3). The ROC analysis results for IVIM parameters in the differential diagnosis of early and late-stage tumors are shown in Table 4.

Assessment of IVIM parameters in differentiation of metastatic from non-metastatic lymph nodes

In surgical patients (n = 18), metastatic lymph nodes were detected in eight patients. The remaining 10 patients had non-metastatic lymph nodes. In patients with metastatic lymph nodes (n = 8), a total of 24 metastatic lymph nodes were identified in the surgical specimens. These metastatic lymph nodes were retrospectively evaluated on conventional MRI according to their location described in the histopathological report. In patients with non-metastatic lymph nodes, the lymph nodes greater than 0.5 mm were also retrospectively reviewed on conventional MRI. Subsequently, a total of 43 (metastatic [n = 24, 56%] and non-metastatic [n = 19, 44%]) lymph nodes were analyzed retrospectively.

In metastatic lymph nodes, D, D^*, and ADC values were lower than those of non-metastatic ones ($p < 0.05$) (Table 5). The ROC analysis and optimal cut-off values of IVIM parameters in the differentiation of metastatic from non-metastatic lymph nodes are shown in Table 6.

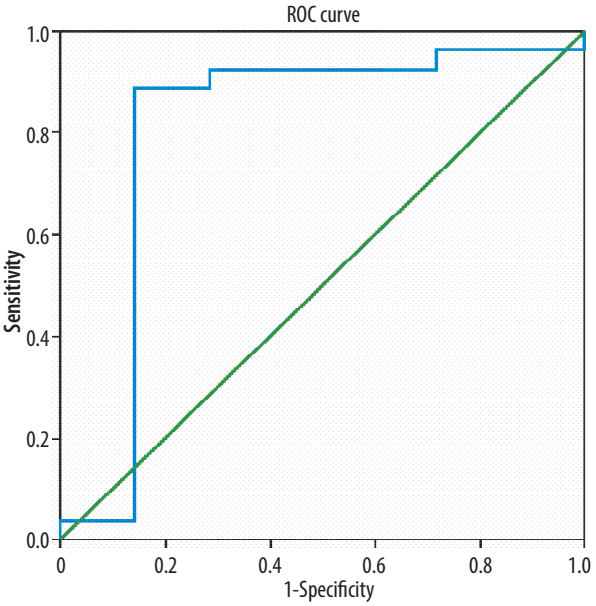

Figure 3. Receiver operating characteristic (ROC) analysis of f value in differentiation of well- and moderately from poorly differentiated tumors

Discussion

Pre-operative imaging is essential for appropriate treatment planning in patients with rectal carcinoma. In routine abdominal MRI, tumoral involvement, the presence of lymphadenopathy, and adjacent organ invasion can be precisely detected [16-19]. However, advances in technology have enabled functional MRI to provide quantitative insights into tumor microstructure beyond morphological characteristics. DWI has made constructive contributions to the depiction of biological behavior in different cancer types [20-22]. There-

Table 2. Distribution of patients according to local invasion degrees

T staging	Local invasion	Operated (n = 18)	Inoperable (n = 9)
Early stage (n = 6, 22.2%)	Submucosal (T1)	4 (14.8%)	–
	Muscularis propria (T2)	2 (7.4%)	–
Late stage (n = 21, 77.8%)	Serosa (T3)	10 (37%)	1 (3.7%)
	Adjacent organ (T4)	2 (7.4%)	8 (29.6%)

Table 3. Comparison of intravoxel incoherent motion (IVIM) diffusion-weighted imaging parameters between early and late stage rectal cancers

IVIM parameter	Early stage (T1-T2)	Late stage (T3-T4)	p*
D ($\times 10^{-3}$ mm^2/s)	1.344 ± 0.294	1.001 ± 0.232	0.013
D^* ($\times 10^{-3}$ mm^2/s)	14.719 ± 3.430	10.97 ± 3.150	0.011
f (%)	26.26 ± 11.99	24.39 ± 5.81	0.929
ADC ($\times 10^{-3}$ mm^2/s) (b = 1000 mm^2/s)	1.660 ± 0.215	1.273 ± 0.241	0.007
ADC ($\times 10^{-3}$ mm^2/s) (b = 1500 mm^2/s)	1.491 ± 0.196	1.137 ± 0.220	0.016

*Mann-Whitney U test; $p < 0.05$ was considered statistically significant.

Table 4. Receiver operating characteristic analysis results for intravoxel incoherent motion (IVIM) parameters in differential diagnosis of early- and late-stage tumors

IVIM parameter	Cut-off value ($\times 10^{-3}$ mm^2/s)	Sensitivity (%)	Specificity (%)	AUC ± SD (95% CI)[a]	*p**
D value	1.17	83.3	80	0.833 ±0.088 (0.660-0.981)	0.015
*D** value	13.71	85	83.3	0.842 ±0.137 (0.573-0.964)	0.013
ADC value ($b = 1000$ mm^2/s)	1.433	92	75	0.858 ±0.085 (0.712-0.993)	0.009
ADC value ($b = 1500$ mm^2/s)	1.132	83	70	0.825 ±0.084 (0.661-0.989)	0.018

[a]Area under the curve ± standard deviation (95% confidence interval). *$p < 0.05$ was considered statistically significant.

Table 5. Comparison of intravoxel incoherent motion diffusion-weighted imaging parameters between metastatic and non-metastatic lymph nodes

Parameter	Metastatic lymph nodes	Non-metastatic lymph nodes	*p**
D ($\times 10^{-3}$ mm^2/s)	0.743 ± 0.112	1.017 ± 0.286	0.001
*D** ($\times 10^{-3}$ mm^2/s)	10.62 ± 4.68	21.37 ± 13.86	0.001
f (%)	33.20 ± 11.44	26.99 ± 8.71	0.055
ADC ($\times 10^{-3}$ mm^2/s) ($b = 1000$ mm^2/s)	1.123 ± 0.252	1.399 ± 0.358	0.016
ADC ($\times 10^{-3}$ mm^2/s) ($b = 1500$ mm^2/s)	0.935 ± 0.221	1.199 ± 0.381	0.008

*Mann-Whitney *U* test; $p < 0.05$ was considered statistically significant.

Table 6. Receiver operating characteristic analysis and cut-off values of intravoxel incoherent motion (IVIM) parameters in differentiation of metastatic from non-metastatic lymph nodes

IVIM parameters	Cut-off value ($\times 10^{-3}$ mm^2/s)	Sensitivity (%)	Specificity (%)	AUC ± SD (95% CI)[a]	*p**
D value	0.936	74	96	0.795 ± 0.071 (0.662-0.928)	0.001
*D** value	12.7	74	83	0.827 ± 0.064 (0.704-0.950)	0.001
ADC value ($b = 1000$ mm^2/s)	1.205	70	73	0.680 ± 0.084 (0.521-0.839)	0.016
ADC value ($b = 1500$ mm^2/s)	1.07	73	88	0.739 ± 0.079 (0.591-0.887)	0.008

[a]Area under the curve ± standard deviation (95% confidence interval). *$p < 0.05$ was considered statistically significant.

fore, the influence of IVIM-DWI parameters in the staging of rectal carcinoma and the determination of tumoral aggressiveness was analyzed in our study. Moreover, a significant relationship was found between histopathological findings and IVIM-DWI parameters.

Our study focused on the relationship between histopathological differentiation and perfusion fraction. Higher *f* values were obtained in well- and moderately differentiated tumors than in poorly differentiated tumors. The *f* value, as an indicator of microcapillary circulation, reveals tumoral aggressiveness and growth potential. Well- and moderately differentiated tumors have more regular microvascular structures, which are associated with higher *f* values; in poorly differentiated tumors, a greater tumoral growth rate results in insufficient microcapillary development, leading to lower *f* values. Lu *et al.* [23] reported a negative relationship between tumoral differentiation and *f* value. In a previous study, lower *f* values in poorly differentiated tumors were associated with inadequate microvascular development [24]. Sun *et al.* [25] reported that poorly differentiated tumors showed lower *f*, *D**, and *ADC* values. Our results align with previous studies and demonstrate that the f value can provide information about tumoral differentiation. In addition, our findings suggest that the perfusion fraction may contribute to preoperative risk stratification, as higher *f* values reflect a more preserved tumor microvasculature, characteristic of better-differentiated lesions.

In evaluating the relationship between tumor extension and IVIM parameters, late-stage (T3-T4) tumors compared to early-stage (T1-T2) tumors had lower *D*, *D**, and *ADC* values, indicating decreased diffusion due to tumoral hypercellularity. In our study, among IVIM parameters and *ADC* values, sensitivity, specificity, and diagnos-

tic performance were highest with the mono-exponential model at *b* values of 0 and 1000 s/mm². A previous study investigated the relationship between tumoral invasion and IVIM parameters. It revealed that lower *D* and *D** parameters were related to increasing tumoral stages [25]. A similar study reported that *D*, *D**, and *ADC* parameters are negatively correlated with tumoral invasion degree [24]. Moreover, other previous studies have shown that a higher invasion degree of rectal cancer showed lower *ADC* values [26-28]. One study showed that the *ADC* map achieved by $b = 1000$ s/mm² achieved the best diagnostic performance in detecting the relationship between tumoral invasion and *ADC* values [29]. Similarly, our results for the *ADC* map at $b = 1000$ s/mm² are consistent with the literature. These results reinforce previous observations and indicate that both *ADC* ($b = 1000$ s/mm²) and *D* values may serve as useful biomarkers in differentiating early- and late-stage rectal carcinoma.

The determination of metastatic lymph nodes has an important role in the staging of rectal cancer. In our study, metastatic lymph nodes had significantly lower *D*, *D**, and *ADC* values compared to non-metastatic lymph nodes. This finding supports the hypothesis that tumoral cellularity restricts diffusion in both the primary tumor and metastatic lymph nodes. Yu *et al.* [30] demonstrated that lower *D* and *D** values were obtained in metastatic lymph nodes. Additionally, in the literature, most studies on metastatic lymph nodes across different malignancies reported lower *ADC* values [31-33]. Taken together, these findings suggest that IVIM-derived parameters may complement conventional MRI for nodal stratification, especially when radiological criteria alone are insufficient.

This prospective study has some limitations. A small sample size was one of them. Additionally, in patients who received neoadjuvant chemotherapy but did not undergo surgery, IVIM parameters may still be influenced by residual treatment-related alterations in perfusion and diffusion characteristics, even if imaging is performed after a standard waiting period. Since the present work was not designed to assess the impact of neoadjuvant therapy on IVIM metrics, no dedicated subgroup analysis was performed. Moreover, in clinically inoperable T4 patients, staging and invasion assessment relied on conventional MRI rather than histopathology, potentially introducing classification bias. Another limitation is that lymph node analysis was performed at the lesion rather than the patient level, which may introduce intra-patient clustering effects in cases with multiple lymph nodes originating from the same subject. Finally, IVIM measurements were performed by consensus readings, and interobserver variability was not evaluated; therefore, potential observer-dependent differences could not be assessed. Further prospective studies with large populations are recommended.

In conclusion, aggressive tumors with low histological differentiation and metastatic lymphadenopathy exhibit lower diffusion and perfusion values. As a perfusion indicator, the *f* value provides valuable findings about tumoral differentiation. IVIM-DWI can be used as an adjunctive modality to routine abdominal MRI in the pre-operative assessment of rectal non-mucinous adenocarcinoma.

Disclosures

1. Institutional review board statement: All procedures performed in studies involving human participants were in accordance with the ethical standards of the institutional and/or national research committee and with the 1964 Helsinki Declaration and its later amendments or comparable ethical standards. The study protocol was approved by Umraniye Training and Research Hospital Institutional Clinical Research Ethics Committee (Decision number: 87, Date: 16.05.2018).
2. Assistance with the article: None.
3. Financial support and sponsorship: None.
4. Conflicts of interest: None.

References

1. Siegel RL, Wagle NS, Cercek A, Smith RA, Jemal A. Colorectal cancer statistics, 2023. CA Cancer J Clin 2023; 73: 233-254.
2. Petrelli F, Tomasello G, Borgonovo K, Ghidini M, Turati L, Dallera P, et al. Prognostic survival associated with left-sided vs right-sided colon cancer. JAMA Oncol 2017; 3: 211.
3. Lehtonen TM, Koskenvuo LE, Lepistö AH. Early-onset rectal cancer: experience of a single-center, high-volume unit. Scand J Surg 2025; 114: 22-34.
4. Hu S, Peng Y, Wang Q, Liu B, Kamel I, Liu Z, et al. T2*-weighted imaging and diffusion kurtosis imaging (DKI) of rectal cancer: correlation with clinical histopathologic prognostic factors. Abdom Radiol 2022; 47: 517-529.
5. Unal OU, Akay S, Semiz HS, Keser M, Demir G, Capar ZG, et al. Survival outcomes according to the tumor location and prognostic factor in metastatic rectal cancer: a multicenter retrospective cohort study. Front Oncol 2024; 14: 1363305.
6. Beets-Tan RGH, Lambregts DMJ, Maas M, Bipat S, Barbaro B, Caseiro-Alves F, et al. Magnetic resonance imaging for the clinical management of rectal cancer patients: recommendations from the 2012 European Society of Gastrointestinal and Abdominal Radiology (ESGAR) consensus meeting. Eur Radiol 2013; 23: 2522-2531.
7. Boss MA, Malyarenko D, Partridge S, Obuchowski N, Shukla-Dave A, Winfield JM, et al. The QIBA profile for diffusion-weighted MRI: apparent diffusion coefficient as a quantitative imaging biomarker. Radiology 2024; 313: e233055.
8. Zeilinger MG, Lell M, Baltzer PAT, Dörfler A, Uder M, Dietzel M. Impact of post-processing methods on apparent diffusion coefficient values. Eur Radiol 2017; 27: 946-955.

9. Le Bihan D, Breton E, Lallemand D, Aubin ML, Vignaud J, Laval-Jeantet M. Separation of diffusion and perfusion in intravoxel incoherent motion MR imaging. Radiology 1988; 168: 497-505.
10. Le Bihan D. Intravoxel incoherent motion perfusion MR imaging: a wake-up call. Radiology 2008; 249: 748-752.
11. Meng X, Tian S, Zhang Q, Chen L, Lin L, Li J, et al. Improved differentiation between stage I-II endometrial carcinoma and endometrial polyp with combination of APTw and IVIM MR imaging. Magn Reson Imaging 2023; 102: 43-48.
12. Cheng Q, Ren A, Xu X, Meng Z, Feng X, Pylypenko D, et al. Application of DKI and IVIM imaging in evaluating histologic grades and clinical stages of clear cell renal cell carcinoma. Front Oncol 2023; 13: 1203922.
13. Chai Y, Niu Y, Cheng R, Gao J. Dynamic contrast enhanced MRI combined with intravoxel incoherent motion in quantitative evaluation for preoperative risk stratification of resectable rectal adenocarcinoma. Oncol Lett 2024; 29: 68.
14. Bai B, Cui L, Chu F, Wang Z, Zhao K, Wang S, et al. Multiple diffusion models for predicting pathologic response of esophageal squamous cell carcinoma to neoadjuvant chemotherapy. Abdom Radiol 2024; 49: 4216-4226.
15. Emir SN, Kulali F, Tosun I, Bukte Y. Predictive intravoxel incoherent motion diffusion-weighted imaging (IVIM-DWI) parameters in the staging of fibrosis in hepatitis B patients. Pol J Radiol 2025; 90: e66-e73.
16. Bedrikovetski S, Dudi-Venkata NN, Kroon HM, Traeger LH, Seow W, Vather R, et al. A prospective study of diagnostic accuracy of multidisciplinary team and radiology reporting of preoperative colorectal cancer local staging. Asia Pac J Clin Oncol 2023; 19: 206-213.
17. Arndt K, Vigna C, Kaul S, Fabrizio A, Cataldo T, Smith M, et al. Magnetic resonance imaging accuracy in staging early and locally advanced rectal cancer. Surg Oncol. 2023;50:101987.
18. Jr LD, Danihel L, Rajcok M, Mosna K, Belan V, Varga I, et al. Significance of MRI in rectal carcinoma therapy optimization – correlation of preoperative T- and N-staging with definitive histopathological findings. Neoplasma 2019; 66: 494-498.
19. Bipat S, Glas AS, Slors FJM, Zwinderman AH, Bossuyt PMM, Stoker J. Rectal cancer: local staging and assessment of lymph node involvement with endoluminal US, CT, and MR imaging – a meta-analysis. Radiology 2004; 232: 773-783.
20. Turkbey B, Rosenkrantz AB, Haider MA, Padhani AR, Villeirs G, Macura KJ, et al. Prostate Imaging Reporting and Data System Version 2.1: 2019 Update of Prostate Imaging Reporting and Data System Version 2. Eur Urol 2019; 76: 340-351.
21. Zhang L, Tang M, Min Z, Lu J, Lei X, Zhang X. Accuracy of combined dynamic contrast-enhanced magnetic resonance imaging and diffusion-weighted imaging for breast cancer detection: a meta-analysis. Acta Radiol 2016; 57: 651-660.
22. Tang L, Zhou XJ. Diffusion MRI of cancer: from low to high b-values. J Magn Reson Imaging 2019; 49: 23-40.
23. Lu B, Yang X, Xiao X, Chen Y, Yan X, Yu S. Intravoxel incoherent motion diffusion-weighted imaging of primary rectal carcinoma: correlation with histopathology. Med Sci Monit 2018; 24: 2429-2436.
24. Zhou B, Zhou Y, Tang Y, Bao Y, Zou L, Yao Z, et al. Intravoxel incoherent motion MRI for rectal cancer: correlation of diffusion and perfusion characteristics with clinical-pathologic factors. Acta Radiol 2023; 64: 898-906.
25. Sun H, Xu Y, Song A, Shi K, Wang W. Intravoxel incoherent motion MRI of rectal cancer: correlation of diffusion and perfusion characteristics with prognostic tumor markers. AJR Am J Roentgenol 2018; 210: W139-W147.
26. Ao W, Bao X, Mao G, Yang G, Wang J, Hu J. Value of apparent diffusion coefficient for assessing preoperative T staging of low rectal cancer and whether this is correlated with Ki-67 expression. Can Assoc Radiol J 2020; 71: 5-11.
27. Peng Y, Tang H, Hu X, Shen Y, Kamel I, Li Z, et al. Rectal cancer invasiveness: whole-lesion diffusion-weighted imaging (DWI) histogram analysis by comparison of reduced field-of-view and conventional DWI techniques. Sci Rep 2019; 9: 18760.
28. Sun D, Wu X, Wang L, Guangzheng G, Huang J, Li Y. Distinguishing T1-2 and T3a tumors of rectal cancer with texture analysis and functional MRI parameters. Diagn Interv Radiol 2022; 28: 200-207.
29. Chen L, Shen F, Li Z, Lu H, Chen Y, Wang Z, et al. Diffusion-weighted imaging of rectal cancer on repeatability and cancer characterization: an effect of b-value distribution study. Cancer Imaging 2018; 18: 43.
30. Yu X ping, Wen L, Hou J, Bi F, Hu P, Wang H, et al. Discrimination between metastatic and nonmetastatic mesorectal lymph nodes in rectal cancer using intravoxel incoherent motion diffusion-weighted magnetic resonance imaging. Acad Radiol 2016; 23: 479-485.
31. He XQ, Wei LN. Diagnostic value of lymph node metastasis by diffusion-weighted magnetic resonance imaging in cervical cancer. J Cancer Res Ther 2016; 12: 77.
32. Razek AAKA, Lattif MA, Denewer A, Farouk O, Nada N. Assessment of axillary lymph nodes in patients with breast cancer with diffusion-weighted MR imaging in combination with routine and dynamic contrast MR imaging. Breast Cancer 2016; 23: 525-532.
33. Yasui O, Sato M, Kamada A. Diffusion-weighted imaging in the detection of lymph node metastasis in colorectal cancer. Tohoku J Exp Med 2009; 218: 177-183.